

Simulation of Dynamic Model of PMFC Using Computer Controlled Power Rectifier for High- Power Applications

DibinChandran

St.Thomas College of Engineering And Technology

Kerala, India

Abstract

This paper presents the guidelines for simulation of dynamic electrical terminal model of a proton exchange membrane (PEM) fuel cell stacks by using a computer-controlled power converter, which drives actual electric loads, or feed power to the grid. The characteristics of simulator include the membrane temperature and efficiency, humidity, flow of the reactants, cooling air fan and water pumps, air environmental and humidity, and regimen of operation of the actual electrical load. Any ordinary size FC of can be simulated without having to use hydrogen with improved safety, variety of tests, demo facility, and flexibility. These features allied to the low cost of this FC simulator contribute for market analysis and life-cycle studies of a site installation.

Index Terms—Computer control, fuel cells(FCs), interconnection, Alternative energy, modeling, rectifiers.

1. Introduction

Fuel cell systems offer clean and efficient energy production and are currently under intensive development by several manufacturers for both stationary and mobile applications. The fuel cell (FC) concept dates back to the early 1800s. Although the

availability and abundance of fossil fuel has limited interest in FCs as a power source, recent advances in membrane and electrode material, reduced usage of noble metal catalysts, efficient power electronics, and electric motors have sparked interest in direct electricity generation using FCs. In particular, proton exchange membranes FCs (PEM-FCs), also known as polymer electrolyte membrane FCs, are most commonly using FC technology. These FCs have high power density, long cell and stack life, solid electrolyte and low corrosion.

PEM-FCs consists of a proton-conducting membrane sandwiched between two platinum-impregnated porous electrodes (membrane electrode assembly, MEA). Hydrogen molecules are split into protons and free electrons at the anode catalyst. The protons diffuse through the membrane to the cathode and react with the supplied oxygen and the returning electrons to produce water. During this process, the electrons pass through an external load circuit and provide useful electric energy. Depending on the catalyst loading a typical PEM-FC provides up to 0.6 W/cm², the membrane and electrode material, and the reactant (oxygen O₂ and hydrogen H₂) concentration in the anode and cathode. To satisfy different power requirements, many FCs are connected electrically in series to form an FC stack (FCS). form an

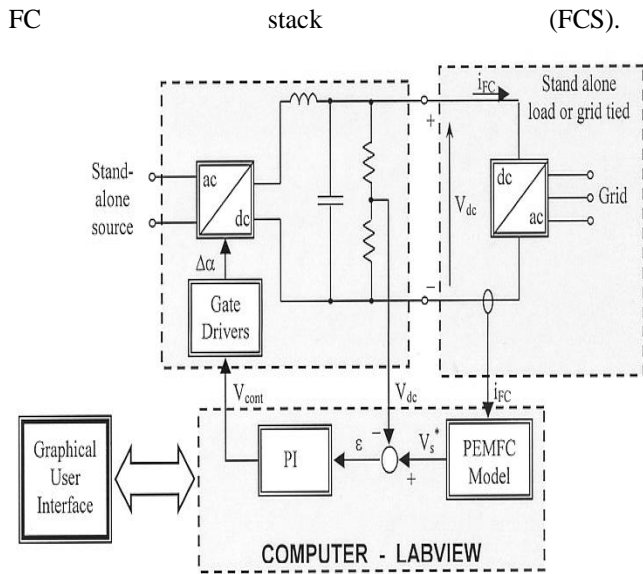


Fig.1 Simulation Block diagram

In particular, proton exchange membrane FC (PEMFC) seems to be a good alternative source for distributed generation systems. Characteristics of PEMFC for such systems: 1) allowing a fast start up with improved dispatch ability because of low temperature operation 2) the by-product is water; 3) they use a solid polymer as the electrolyte, which reduces concerns related to construction, transportation, and safety issues. In present situation high costs of FC stacks make research and development of this type of generation systems a difficult task, especially for developing countries and schools in general. In generating systems there are still some concerns about the FC dynamic behavior, such as its response to fast load changes, peak power, response to nonlinear loads and peak current capabilities. There are also some safety factors about utilization and storage of hydrogen, besides its high price and lack of ready supplying facilities in present scenario.

2. Fuel cell operation and model

Fig. 2 shows the operation of a typical PEM fuel cell. The rightside of the cell shown in Fig. 2 is exposed to

atmospheric oxygen, while the left side of the assembly is exposed to hydrogen from the fuel source. On the fuel side of the FC, hydrogen dissociates in the presence of a catalyst into electrons and H^+ ions. The electrons flow to the external circuit from a current collector. The electron flow is matched by a flow of hydrogen ions, which move readily through the electrolyte. On the air side of the cell, electrons, oxygen and hydrogen ions combine and water and heat produced. The catalyst terminals of the fuel cell are labeled cathode or anode with respect to the ion current flowing in the electrolyte; the positive ionic current originates at the fuel-side anode and flows through the electrolyte to the oxygen-side cathode. Typically, the anode, cathode, and electrolyte are laminated together to form a thin membrane electrode assembly or MEA.

The voltage E developed over a single cell such as that shown in Fig. 2 is ideally described by the Nernst equation

$$E = E_0 + \frac{RT}{2F} \ln \frac{P_{H_2} P_{O_2}^{1/2}}{P_{H_2O}} \quad (1)$$

Here, E_0 is the standard potential of the hydrogen/oxygen reaction (about 1.229 V), R is the universal gas constant, F is Faraday's constant, T is the absolute temperature, and P_{H_2} is the partial pressure of hydrogen available at the anode.

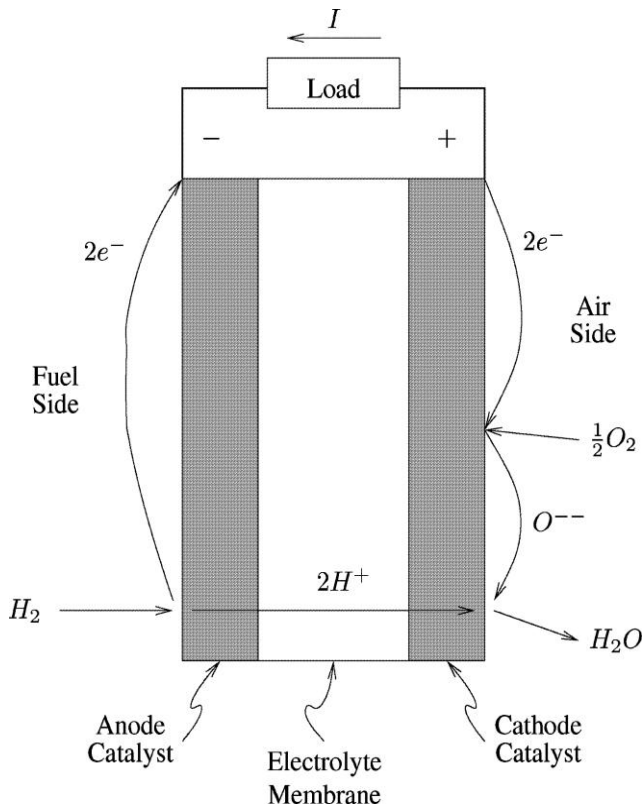


Fig. 2. Conceptual diagram of PEMFC.

Similarly, P_{H_2O} and P_{O_2} are partial pressures of water and oxygen at the cathode. In (1) the partial pressures of species appearing on one side of the chemical reaction appear in the numerator, while the other side of the reaction appears in the denominator. In equilibrium, with no electrical connections, the cell voltage saturates to the standard potential, and the ratio of partial pressures is unity. Under load, the quantities in the numerator are consumed while quantities in the denominator are produced, and the cell voltage drops. The relationship between the last term in (1), built-in potentials in the cell, and the current can be modeled by writing the cell voltage

$$E = E_0 - IR - aT \ln \frac{I}{i_0} - bT \ln \frac{i_L - I}{i_L} \quad (2)$$

In (2), R is a resistance, including the cell internal resistance, I is the terminal current, and a and b lump

terms that can be assumed constant for a particular cell and reaction. Starting from IR , these loss terms are ohmic, the activation over potential, and the concentration over potential. Activation over potential is a loss term associated with energy barriers that must be overcome to start the reaction. Concentration over potential is a loss associated with the depletion of reactants at high currents. Although the exchange current parameter i_0 for activation and the limiting current i_L for depletion depend on the fuel cell, the activation loss typically dominates the response at low currents, while the effect of the concentration overpotential is most obvious at high currents. The response of our SR-12 PEM stack is nearly linear for a useful range of currents between the activation and concentration regions. Expanding (2) in a Taylor series for currents $I = I_0 + \tilde{I}$ yields

$$E = E_0 - (I_0 + \tilde{I})R - aT \left[\ln \frac{I_0}{i_0} + \frac{1}{I_0} \tilde{I} \right] - bT \left[\ln \frac{i_L - I_0}{i_L} - \frac{1}{i_L - I_0} \tilde{I} \right] + \text{higher order terms} \quad (3)$$

where \tilde{I} is a small signal current and I_0 is the operating point. Assuming that the higher order terms in the current perturbation can be ignored and that \tilde{I} and T are the variables of interest, then Writing $T = T_0 + \tilde{T}$, and assuming a stack of n identical cells in series, the stack voltage can be written as

$$V(\tilde{I}, \tilde{T}) = A + B\tilde{T} + C\tilde{I} + D\tilde{I}\tilde{T} \quad (4)$$

where the coefficients in terms of the original parameters are

$$A = n(E_0 - I_0R) + T_0B \quad (5)$$

$$B = -n \left[a \ln \frac{I_0}{i_0} + b \ln \frac{i_L - I_0}{i_L} \right] \quad (6)$$

$$C = -nR + T_0D \quad (7)$$

$$D-n \left[\frac{a}{I_0} + \frac{b}{i_L - I_0} \right] \quad (8)$$

The use of in (4) makes B the sensitivity to temperature change and directly comparable to C, the incremental resistance.

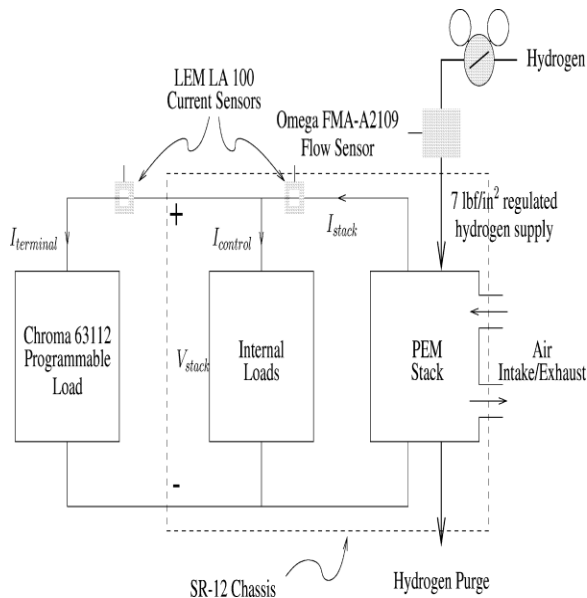


Fig. 3. Schematic of experimental setup.

With this definition, has the interpretation as the perturbation in temperature due to. Subtracting yields

$$\alpha \frac{dT}{dt} = -\tilde{T} + (2\gamma I_0 + \delta)\tilde{I} + \gamma \tilde{I}^2 \quad (9)$$

Rewriting with $\beta = 2\gamma I_0 + \delta$

$$\alpha \frac{dT}{dt} = \tilde{T} + \beta \tilde{I} + \gamma \tilde{I}^2 \quad (10)$$

Where the parameters α , β , and γ in (10) are independent.

3. Model formulation

In order to model an FC stack some parameters are required to fit our model. Although most of the parameters are obtained from the manufacturer's datasheet, a few are still required from experimentation

and from the available literature. In this paper, a model for a 500-W stack, manufactured by BCS Technologies, is used. The parameters for this particular model are presented in [4]. The output voltage of a single cell can be defined as the result of the following expression

$$V_{FC} = E_{Nerst} - V_{act} - V_{Ohmic} - V_{con} \quad (11)$$

In (2), E_{Nerst} is the thermodynamic potential of the cell and it represents its reversible voltage; V_{act} is the voltage drop due to the activation of the anode and of the cathode; V_{Ohmic} is the ohmic voltage drop, a measure of the ohmic voltage drop associated with the conduction of the protons through the solid electrolyte and electrons through the internal electronic resistances; and V_{con} represents the voltage drop resulting from the concentration or mass transportation of the reacting gases

$$E_{Nerst} = 1.229 - 0.85 \times 10^{-3}(T - 298.15) + 4.31 \times 10^{-5} \cdot T \cdot [\ln(pH_2 + \frac{1}{2} \ln(pO_2))] \quad (12)$$

$$V_{act} = -[\varepsilon_1 + \varepsilon_2 \cdot T + \varepsilon_3 \cdot T \cdot \ln(C_{O_2}) + \varepsilon_4 \cdot T \cdot \ln(i_{FC})] \quad (13)$$

$$V_{Ohmic} = i_{FC} \cdot (R_M + R_C) \quad (14)$$

$$V_{con} = -B \cdot \ln(1 - \frac{J}{J_{max}}) \quad (15)$$

Where

C_{O_2} = Concentration of O_2 in the catalytic interface of the cathode (mol/cm³);

C_{H_2} = concentration of H_2 in the catalytic interface of the anode (mol/cm³);

i_{FC} = FC actual current (A);

R_M = equivalent membrane resistance (Ω);

J =actual FC current density (A/cm²).

The concentration of gas can be calculated using the following equation. For oxygen, for example, we have

$$C_{O_2} = \frac{P_{O_2}}{5.08 \times 10^6 \cdot e^{-\left(\frac{498}{T}\right)}} \quad (16)$$

The equivalent membrane resistance can be calculated by

$$R_M = \frac{\rho M l}{A} \quad (17)$$

Where ρM is the membrane specific resistivity (Ω cm), which can be obtained by

$$\rho M = \frac{181.6 \cdot \left[1 + 0.03 \left(\frac{i_{FC}}{A} \right) + 0.062 \cdot \left(\frac{T}{303} \right)^2 \left(\frac{i_{FC}}{A} \right)^{2.5} \right]}{\left[\psi - 0.634 - 3 \left(\frac{i_{FC}}{A} \right) \right] \cdot \exp \left[4.18 \cdot \left(\frac{T - 303}{T} \right) \right]} \quad (18)$$

where the term $181.6 / (\psi - 0.634)$ is the specific resistivity (Ω cm) at no current and at temperature of 30⁰ C; the exponential term in the denominator is the temperature factor correction if the cell is not at 30⁰C. The parameter ψ is considered an adjustable parameter, with a possible minimum value of 14 and a maximum value of 23

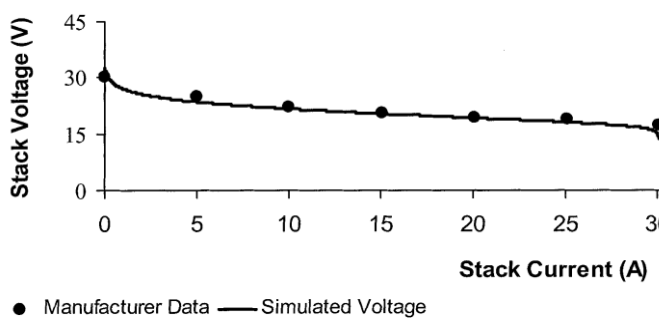


Fig. 4. Polarization curve of the 500-W BCS stack.

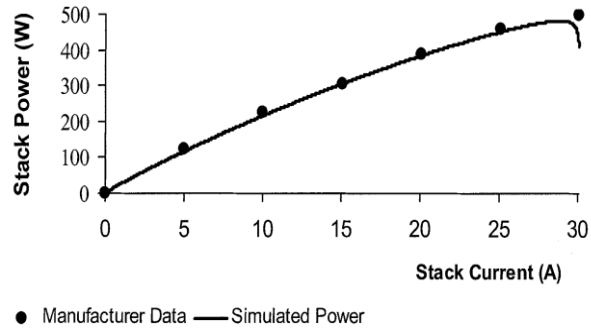


Fig. 5. Power characteristic of the 500-W BCS stack.

Including this electrical dynamic behavior term, the resulting FC voltage is then defined by

$$V_{FC} = E_{Nernst} - v_d - v_{ohmic} \quad (19)$$

The polarization curve of an FC represents its output voltage against the load current density (or against the load current). This curve is important because it shows how the FC voltage behaves when the load current changes. However, it is important to note that the polarization curve represents just the cell static operation; because each voltage point in this curve is obtained only after it reaches its steady-state value.

For most parts of the curve in Fig. 4 the results show good agreement. However, at the beginning and at end of the simulation, there is only a poor agreement. The reason for this is the difficulty of finding out the right parameters set for the FC stack.

Fig. 5 presents the stack output power against current, again for the manufacturer’s data and for the simulated data. Except for the end of the simulation, the results again show a good agreement.

In an FC stack supplied with pure hydrogen, the fuel consumption can be obtained by

$$\dot{m}_{H_2O} = 9.34 \times 10^{-8} \cdot \frac{P_s}{V_{FC}} \quad (20)$$

where is the hydrogen mass flow rate (kg/s); is the FC voltage (V), obtained from (19); and is the stack electrical power (W), obtained from

$$P_s = n \cdot V_{FC} \cdot i_{FC} \quad (21)$$

where is the number of cells used on the stack.

The air mass flow rate (kg/s) can be obtained using

$$\dot{m}_{ar} = 3.57 \times 10^{-7} \cdot \lambda \cdot \frac{P_s}{V_{FC}} \quad (22)$$

where is the stoichiometric rate.

Finally, the rate of water production, in kg/s, in a stack operation is calculated by

$$\dot{m}_{H_2O} = 9.34 \times 10^{-8} \cdot \frac{P_s}{V_{FC}} \quad (23)$$

4. Experimental results

The following results are based on the loading insertion/rejection tests, using the 500-W BCS stack modeling. An overall test was run in order to analyze the stack performance against variations of an ordinary real load. The load used in the following tests consists of a variable resistance at a maximum value of 750 , which allows the simulator output power to vary from practically no load to full load. The load current waveform of the test is shown in Fig. 6. The maximum value is about 1.5 A and it was applied for a period of about 20 s. Fig. 7 shows the computer simulated stack voltage, which is the reference voltage. Fig. 8 shows the converter output voltage, which corresponds to the voltage applied to the load.

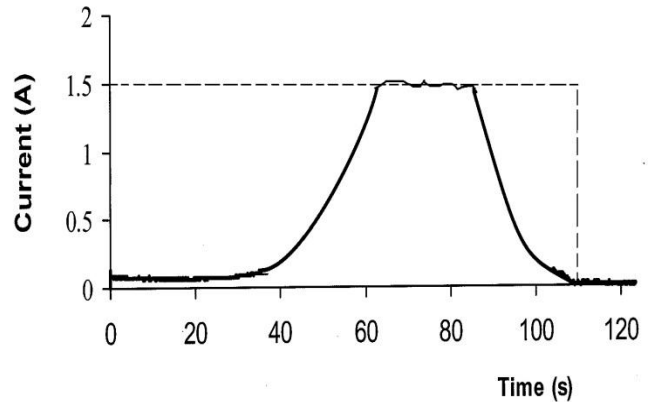


Fig. 6. Actual load current for insertion/rejection test.

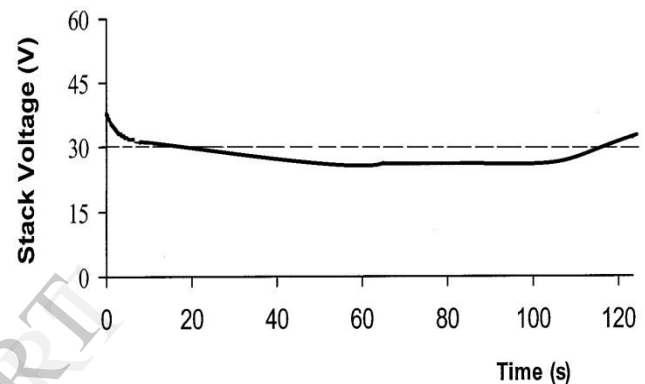


Fig. 7. Reference voltage, representing the stack output voltage.

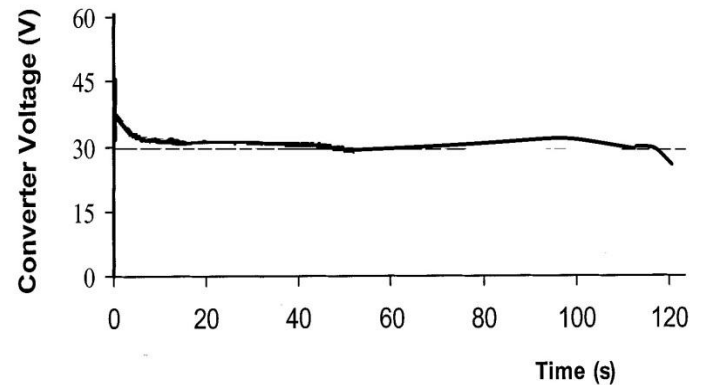


Fig. 8. Converter output voltage.

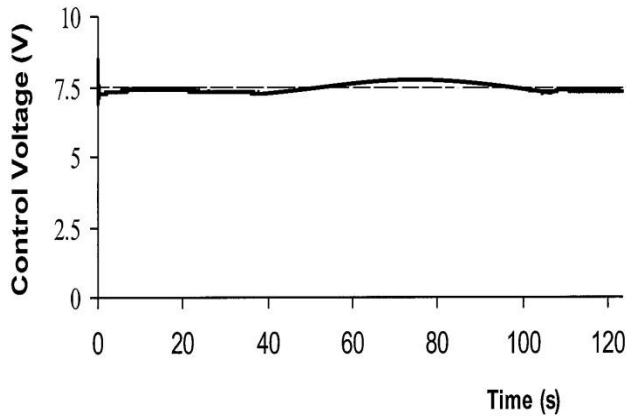


Fig. 9. Controller output signal.

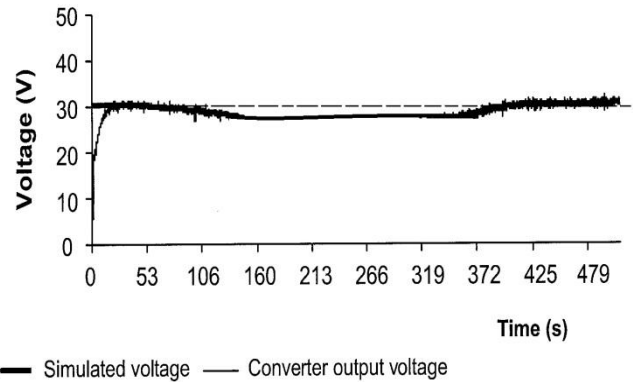


Fig. 12. Output voltage from simulated stack and from converter.

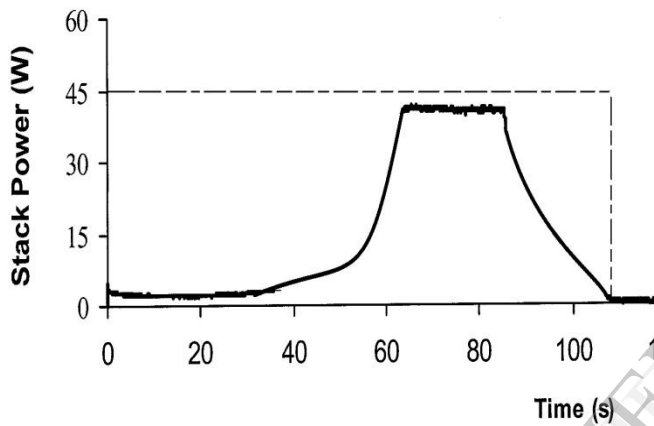


Fig. 10. Simulated stack output power.

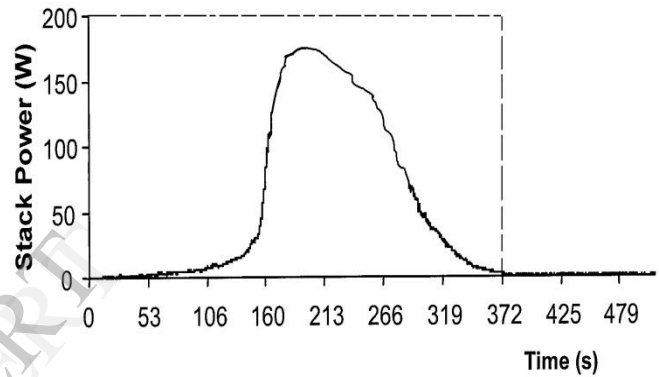


Fig. 13. Simulated FC output power.

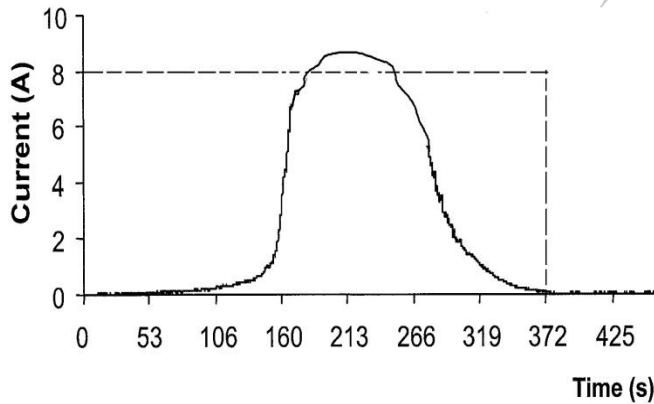


Fig. 11. Actual FC load current.

Figs. 7 and 8 shows that there is a voltage drop when the load current increases. This voltage drop is about 6 V, from a no-load condition to a current load of 1.5 A. This dynamic behavior was considered by using (1)–(12). Also, it should be noted that, even for this small load current, there is a significant voltage drop. Comparing the two curves, one can see that the converter output voltage presents a good agreement with the reference voltage. The signal of the converter controller is shown in Fig. 9. The curve presents a soft shape, showing relatively good control performance. Fig. 10 presents the simulated stack output power for this test. The maximum power is about 40W. The resulting stack efficiency for this power is about 52%. It can be considered a high

efficiency, but one should note that the power in this case is just 8% of the full power.

The following results were obtained for a higher load current, to evaluate the stack behavior in such a situation. The load current for this test is shown in Fig. 11 and the comparison between the simulated stack voltage and the converter output voltage is presented in Fig. 12. For this test it is possible to observe that the converter voltage presents some more noticeable oscillation at instants of quick load changes, about 160 and 270 s. This response is characteristic of the passive LC filters used in controlled power converters working as a voltage source to supply resistive loads.

The power supplied to the load in this test is presented in Fig. 13, with a maximum value of about 180 W, corresponding to 36% of the full load. Even at this higher power, the stack behaves almost the same as for the lower current. Therefore, the FC-Sim can be used to evaluate low-power and high-power situations, making it a versatile tool for analysis of FC systems.

5. Conclusion

This paper provides a family of models that accurately describe PEM dynamic behavior, even on cross-validation. Although developed with a small-signal formalism, the models appear to be useful for wide-ranging current and voltage responses with our SR-12 test fuel cell.

The power converter acted as a voltage-controlled source, supplying the load with the same power as the actual simulated FC stack. The simulated results agreed within less than 3% with the results presented in the current manufacturer's datasheet for the polarization curve. The dynamic behavior of a specific set of FC stacks was analyzed using the FC-Sim simulator. Results for the η -characteristic showed clearly the expected output voltage dependence on the load current. The converter output voltage has shown good agreement with

the stack reference voltage, as a result of the PI controller performance. However, at points of quick load changes, some voltage oscillation across the load terminals was noticed. These oscillations were caused by the natural converter response. Taking the results presented in this paper into account, the developed simulator prototype seemed to be suitable for laboratory tests as it may help development of stack power control algorithms, dedicated power converters for power injection into the grid, online market analysis, as well as being an aid in developing FC operation control methods.

References

- [1] J. M. Corrêa, F. A. Farret, and L. N. Canha, "An analysis of the dynamic performance of proton exchange membrane fuel cells using an electromechanical model," in Proc. IEEE IECON'01, 2001, pp. 141–146.
- [2] J. Padullés, G. W. Ault, and J. R. McDonald, "An integrated SOFC plant dynamic model for power systems simulation," *J. Power Sources*, vol. 86, pp. 495–500, Mar. 2000.
- [3] J. J. Baschuck and X. Li, "Modeling of polymer electrolyte membrane fuel cells with variable degrees of water flooding," *J. Power Sources*, vol. 86, pp. 181–196, 2000.
- [4] D. J. Hall and R. G. Colclaser, "Transient modeling and simulation of a tubular solid oxide fuel cell," *IEEE Trans. Energy Convers.*, vol. 14, no. 3, pp. 749–753, Sep. 1999.
- [5] J. Padullés, G.W. Ault, and J. R. McDonald, "An integrated SOFC plant dynamic model for power systems simulation," *J. Power Sources*, vol. 86, pp. 495–500, 2000.
- [6] J. Padullés, G. W. Ault, C. A. Smith, and J. R. McDonald, "Fuel cell plant dynamic modelling for

power systems simulation,” in Proc. 34th Universities Power Engineering Conf., vol. 1, Leicester, U.K., Sep. 1999, pp. 21–25.

Dibin Chandran was born in 30 March 1990 in India. He completed his B.Tech degree from Saintgits College of Engineering, Mahatma Gandhi University, Kerala. He completed his master degree from Karunya University in Renewable Energy Technology. Currently he is working as assistant professor in St.



Thomas College of Engineering and Technology, Kerala. His main interest is in Wind Power, Power Electronics and Fuel Cell.

IJERT